Atmos. Chem. Phys. Discuss., 10, 25205–25242, 2010
www.atmos-chem-phys-discuss.net/10/25205/2010/
doi:10.5194/acpd-10-25205-2010

Atmospheric Chemistry and Physics Discussions

First long-term study of particle number size distributions and new particle formation events of regional aerosol in the North China Plain

X. J. Shen[1], J. Y. Sun[1], Y. M. Zhang[1], B. Wehner[2], A. Nowak[2], T. Tuch[2], X. C. Zhang[1], T. T. Wang[1], H. G. Zhou[3], X. L. Zhang[3], F. Dong[3], W. Birmili[2], and A. Wiedensohler[2]

[1]Key Laboratory for Atmospheric Chemistry, Center for Atmosphere Watch and Services, Chinese Academy of Meteorological Sciences, China Meteorological Administration, Beijing 100081, China
[2]Leibniz Institute for Tropospheric Research, 04318 Leipzig, Germany
[3]Shangdianzi Regional GAW station, Research Institute of Urban Meteorology, Beijing Meteorological Bureau, Beijing 100089, China

Received: 8 October 2010 – Accepted: 11 October 2010 – Published: 28 October 2010

Correspondence to: J. Y. Sun (jysun@cams.cma.gov.cn)

Published by Copernicus Publications on behalf of the European Geosciences Union.

Abstract

Atmospheric particle number size distributions (size range 0.003–10 µm) were measured between March 2008 and August 2009 at Shangdianzi (SDZ), a rural research station in the North China Plain. These measurements were made in an attempt to better characterize the tropospheric background aerosol in Northern China, one of the currently more polluted regions of the globe. The mean particle number concentrations of the total aerosol, as well as the nucleation, Aitken and accumulation modes were determined to $1.2\pm0.9\times10^4$, $3.6\pm7.9\times10^3$, $4.4\pm3.4\times10^3$ and $3.5\pm2.8\times10^3$ cm^{-3}, respectively. A general finding is that the particle number concentrations were higher during spring compared to the other seasons. The air mass origin had an important effect on the particle number concentration and new particle formation events. Air masses from northwest (i.e. inner Asia) showed the highest concentrations of nucleation mode particles, while southeasterly air masses showed the highest concentrations of accumulation mode particles. Significant diurnal variations in particle number were observed, which could be linked to new particle formation events, i.e. gas-to-particle conversion. During particle formation events, the number concentration of the nucleation mode rose up to maximum values of 10^4 cm^{-3}. New particle formation events were observed on 36% of the measurement days. The formation rate ranged between 0.7 and 72.7 cm^{-3} s^{-1}, with a mean value of 8.0 cm^{-3} s^{-1}. The values of the nucleation mode growth rate ranged between 0.3 and 14.5 nm h^{-1}, with a mean value of 4.3 nm h^{-1}. It is an essential observation that on many occasions, the nucleation mode was able to grow into the size of cloud condensation nuclei (CCN) within a matter of several hours. Furthermore, the new particle formation were usually followed by a measurable increase in total particle mass concentration and extinction coefficient, indicative of a high abundance of condensable vapors in the atmosphere under study.

ACPD
10, 25205–25242, 2010

1 Introduction

Atmospheric aerosol particles play a key role in global climate because of combined direct and indirect radiative forcing. They directly affect the radiation balance by scattering and absorbing incoming short-wave solar radiation and absorbing long-wave radiation. Indirectly, aerosol particles have a substantial effect on cloud properties and the initiation of precipitation as cloud condensation nuclei (CCN) (Rosenfeld et al., 2008). The scattering and absorption of light by particles can effect atmospheric visibility (Middleton, 1952). Evidences from medical studies indicate that air pollution is a major contributor to cardiovascular and respiratory health problems (Hong et al., 2002). Hospital admissions and emergency room visits for cardiovascular and respiratory diseases are increasing with the elevated ambient particle concentrations (Dominici et al., 2006). Growing knowledge regarding interconnected general pathophysiological pathways those link PM exposure with cardiopulmonary morbidity, especially mortality exposure to fine particulate air pollution (Pope III and Dockery, 2006). The number size distribution is an important characteristic, which can help to understand the behavior and effects of the aerosol particles (Birmili et al., 2001). Particle number size distributions can be measured down to sizes as small as 3 nm in diameter with high time resolution due to recent developments in instrumentation (Kulmala et al., 2004), but the latest developments have extended detection limits to sizes below 2 nm (Kulmala et al., 2007; Iida et al., 2008; Sipilä et al., 2009).

Ground-based in-situ measurements of aerosol properties such as size distribution, chemical composition, scattering and absorption coefficient were performed at a number of sites, either at long-term monitoring sites, or as part of intensive field campaigns (IPCC, 2007). A wide body of in-situ observations of tropospheric aerosols have been made in urban and rural areas in Europe and North America, e.g., Birmingham (Harrison et al., 1999), Atlanta (Woo et al., 2001), Helsinki (Hussein et al., 2004), Leipzig (Birmili et al., 2001; Wehner and Wiedensohler, 2003), Pittsburgh (Stanier et al., 2004). During the recent years, efforts have been made to characterize particle number size

ACPD
10, 25205–25242, 2010

distributions in developing countries as well, because their air pollution problems are of significant local and even global concern, such as in New Delhi (Laakso et al., 2005) and Beijing (Wu et al., 2008).

The formation of new particles in the atmosphere and its effects on the budget of the number concentration of submicrometer particles are a vital issue in atmospheric science (e.g., Seinfeld and Pandis, 1998). Particle formation increases the total number concentration of ambient submicrometer size particles and thereby effecting climate forcing and human health (Twomey, 1977). Measurements of particle size distributions revealed new particle formation (NPF) events and growth are widespread. Kulmala et al. (2004) concluded that the formation rate of 3 nm particles is often in the range 0.01–10 $cm^{-3}\,s^{-1}$ in the boundary layer. However, in urban areas formation rates are often higher than this (up to 100 $cm^{-3}\,s^{-1}$), and rates as high as 10^4–10^5 $cm^{-3}\,s^{-1}$ were observed in coastal areas and industrial plumes. Typical particle growth rates are in the range 1–20 $nm\,h^{-1}$ in mid-latitudes depending on the temperature and the availability of condensable vapors. The studies show that sulfuric acid plays a dominant role in new particle formation and growth (Boy et al., 2005; Riipinen et al., 2007), and organic compounds have also been thought to have the potential role (Zhang et al., 2004; Barsanti et al., 2009). Condensation and coagulation are also important for new particle formation events. Low condensation sink favors nucleation because in this case the particle growth from ~1–3 nm is possible before their coagulation with larger particles (Hamed et al., 2007). Coagulation has an effect on reducing nucleation mode particle number concentration (Kerminen and Kumala, 2002). Condensation of sulfuric acid and coagulation both contribute to the particle growth after nucleation (Kerminen and Kumala, 2002; Yue et al., 2010).

In China, particle number size distribution measurements were carried out in few places only. Short term measurements of particle number size distribution were performed in Pearl River Delta (Liu et al., 2008; Yue et al., 2009), a suburban site in the Yangtze River Delta (Gao et al., 2009) and vertical ultrafine particles profiles over Northern China coastal areas (Wang et al., 2008). Long term measurements were only

ACPD
10, 25205–25242, 2010

carried out in Beijing (Wu et al., 2008) and a remote mountain-top station, Waliguan (Kivekäs et al., 2009). There is however no data about long-term measurements of particle number size distribution of the regional polluted aerosol in China yet. Thus, information on the long-term behavior of particle number size distributions is still sparse.

As a part of EUCAARI (European Integrated project on Aerosol Cloud Climate and Air Quality Interactions), joint research measurement are conducted at Shangdianzi (SDZ) regional background station by the Leibniz Institute of Tropospheric Research and Chinese Academy of Meteorological Sciences since 2008, in order to better understand the chemical and physical characteristics of atmospheric aerosols over the North China Plain. This paper focuses on the size distribution measurements at SDZ from March 2008 to August 2009, and summarizes the characteristics of particle number concentration, size distribution and new particle formation events at SDZ.

2 Experimental

2.1 Measurements site

Shangdianzi (SDZ) regional background station is one of the regional Global Atmosphere Watch (GAW) stations in China and also one station of National Atmospheric Composition Background observation and Research station system of China. It is located in the northern part of North China Plain; about 55 km and 150 km northeast of the urban areas of Miyun and Beijing, respectively. Surrounding the site, there are rolling hills with farmland, orchards and forest. On the foot of the hills about 2 km south of the station is Shangdianzi village with about 1200 inhabitants and a small factory for screw casting. The major local economical activities within Miyun County are farming and fruit growing (Yan et al., 2008). The closest town nearby is Gubeikou which is in northwest of SDZ and 5 km away, besides, a national highway opened in November 2009 is located in the east about 3 km away. Although there are some local anthropogenic pollution sources surrounding the SDZ site, the amount is quite less

ACPD
10, 25205–25242, 2010

compared to the emission form big cities. The observations at SDZ are representative for the North China plain, especially the Beijing-Tianjin-Hebei (Jing-Jin-Ji) metropolitan region, if the air is originated from South. Figure 1 shows the location of SDZ and some cities around, like Beijing, Tianjin, Tangshan, Shijiazhuang. The northern regions of SDZ are much less inhabited and the industrial activities are less prevalent. The station is located on the north hill side of a valley with a northeast-southwest orientation. The southwest mouth of the valley is open to Beijing and the south plain. Due to the valley topography, the prevailing winds are northeasterly and southwesterly.

2.2 Instrumentation

Particle number size distributions between 3 nm and 10 µm were measured with a time resolution of 10 min about 1.5 year at the rural site, SDZ from March 2008 to August 2009. A twin differential mobility particle sizer (TDMPS) system consisting of two differential mobility analyzers (DMA) and two condensation particle counters (CPCs, model 3010 and model 3025, TSI Inc., St. Paul, USA) was used to measure particle size distributions from 3–850 nm mobility diameter (Birmili et al., 1999). Simultaneously, an aerodynamic particle sizer (APS, model 3321, TSI Inc., St Paul, USA) measured number size distributions of particles with aerodynamic diameter from 700 nm to 10 µm. The resulting distributions of APS system were transformed from aerodynamic to mobility diameters using assumed particle density of 1.7 g cm^{-3}, the same as that used in Beijing study (Wu et al., 2008), as there was no chemical composition measurement data available at SDZ. When the aerodynamic diameter was transferred to mobility diameter, the total size distributions actually covered the size range from 3 nm to 7.7 µm in mobility diameter. Looking at particle number concentrations, the contribution of particles larger than 1 µm is very small and can be ignored. A low flow PM_{10} inlet with dryer was used to supply sample for both systems. The relative humidity within the systems was kept below 30% by adding an automatic regenerating adsorption aerosol dryer in the inlet line (Tuch et al., 2009). It ensures the comparability between different aerosol measurements. An inversion routine to transfer from mobility to diameter

ACPD
10, 25205–25242, 2010

size distributions accounted for the bipolar charge distribution, and empirically determined transfer functions of the DMAs. Size-dependent diffusional losses for the inlet pipe were also corrected by using the empirical functions given by Willeke and Baron (1993). In addition, the individual CPC and UCPC counting efficiencies were considered for data correction. All are subsequently reported for standard pressure and temperature (1013 hPa and 273 K) to provide comparability with other measurements. The time used in this study is Beijing local time (UTC+8 h).

In addition, basic meteorological parameters, such as air temperature, relative humidity, wind speed and wind direction were recorded at the station and used in this investigation.

3 Results and discussion

A continuous 1.5 year dataset was evaluated in this investigation. Except the instrument malfunction and movement, 86% of this period was effective. The continuous dataset of particle number size distributions was integrated to calculate particle number concentrations in different size classes. In this study, diameter ranges for the nucleation mode, Aitken mode, accumulation mode, and coarse mode were chosen as 3–25 nm, 25–100 nm, 100–1000 nm, and 1–10 µm, respectively. The total particle number concentration means particle number concentration from 3 nm to 10 µm. The particle volume and surface area concentrations were calculated from the measured number size distributions assuming spherical particles.

3.1 Overview of the particle number concentration

Nucleation mode particles are formed by condensation and coagulation of the low volatile condensable gases such as sulfuric acid (Kulmala, 2003). Aitken mode particles are directly emitted from combustion processes, such as car traffic, and also result from condensational growth and coagulation of nucleation mode particles. In

ACPD
10, 25205–25242, 2010

urban areas, the traffic emission is a predominant source (Wu et al., 2008), and in rural areas nucleation particles growth is more important (Stanier et al., 2004). Accumulation mode particles originate from coagulation and condensational growth of Aitken mode particles and the air mass long-range transport from polluted areas.

Statistical parameters for nucleation mode (Nnuc), Aitken mode (Nait), accumulation mode (Nacc) particles and the total particle number (Ntot), surface area (Stot), and volume concentrations (Vtot) over the entire measurement period were calculated. The mean values for Nnuc, Nait, Nacc, Ntot are $3.6\pm7.9\times10^3$, $4.4\pm3.4\times10^3$, $3.5\pm2.8\times10^3$ and $1.2\pm0.9\times10^4$ cm^{-3}, respectively. Aitken mode particles are slight higher than the other two modes. The total particle surface area and volume concentrations are 690 μm^2 cm^{-3} and 50 μm^3 cm^{-3}, respectively. During dust storm events, the number of coarse mode particles increases significantly. The maximum of the particle volume concentration was 1560 μm^3 cm^{-3}, which was observed during a typical dust storm event occurred on 18 March 2008.

Table 1 is the comparison between this study and those conducted at other places in different urban and rural environments in China. The mean total number concentration at SDZ is much lower than those in Beiing, 32 800 cm^{-3} (Wu et al., 2008), Shanghai suburban site, 30 187 cm^{-3} (Gao et al., 2009), also lower than those in Jinan city, 10 685–17 387 cm^{-3} (Gao et al., 2007) and some rural sites like Yufa, 17 000 cm^{-3} (Yue et al., 2009) and Xinken, 16 300 cm^{-3} (Liu et al., 2008), but much higher than those at Mt. Waliguan, a global GAW sites in China, 2030 cm^{-3} (Kivekäs et al., 2009). The reason for this somewhat lower total number concentration compared to Yufa (also a regional site in the North China plain) is twofold. First, the data at Yufa cover only a time period of 4 weeks in summer 2006, and second, SDZ is on the border to the mountains in the North with very frequent influence with very clean air. The result of a back trajectory cluster analysis is shown below.

Figure 2 shows the monthly variation of particle number concentrations of nucleation mode (Nnuc), Aitken mode (Nait), accumulation mode (Nacc) and total particles (Ntot), respectively. There are two data gaps because an instruments malfunction in June

ACPD
10, 25205–25242, 2010

2008 and instruments location change in March 2009, where instruments were moved to a lower part of the station, about 750 m away because of construction work. The number concentration of nucleation mode particles (Fig. 2a) showed a clear monthly variation with the minimum mean value about 1000 cm^{-3} in July and August 2008 while the maximum mean value 10 000 cm^{-3} in March 2008. An explanation for this variation was that new particle formation events (NPF) occurred most frequently in spring and least in summer. Due to the newly formed particles growth, the mean number concentration of Aitken mode particles was higher during spring months and lower during summer months (Fig. 2b). The variation of accumulation mode particle number concentrations (Fig. 2c) had the same trend with that of Aitken mode except in fall 2008 and June 2009, because the Aitken mode particles grew by condensation mainly during air mass long-range transportation. The total particle number concentration seemed to be higher during spring months and lower during summer months (Fig. 2d), and the monthly mean concentration varied from about 6000 cm^{-3} to 20 000 cm^{-3}.

3.2 Diurnal variations of particle number size distribution

The diurnal pattern of aerosol number concentration of each mode was investigated separately for different seasons, i.e. spring (March–May), summer (June–August), fall (September–November), and winter (December–February). The seasonal-average number concentration of particles of each mode was calculated using the 10 min resolution data for each season. Figure 3 shows that the diurnal behaviors of particle size distribution (a–d) and different mode particle number concentrations (e–h) vary with seasons. As seen in Fig. 3a, the particle size distribution in spring showed the nucleation mode particles, with the minimum diameter, about 3 nm, appeared at about 08:00 LT, when NPF events started. The freshly nucleated grew to larger sizes due to condensation or coagulation of the existing particles within several hours, contributing to the increase of Aitken mode and accumulation mode particles. Nucleation mode particles almost disappeared until 16:00 LT. The evolution of particle size distribution in spring shows clearly particle formation and growth due to the frequent NPF events. The

ACPD
10, 25205–25242, 2010

meteorological factors like low temperature, low relative humidity, high solar radiation, and low condensation sink (CS) favor the NPF events (Boy et al., 2002). In summertime (Fig. 3b), the nucleation mode particles appeared around 08:00 LT, at about 10 nm, with the possible explanation that the newly formed particles had grown to larger size when detected. Then the particles grew to larger sizes gradually till the end of the day. In fall (Fig. 3c) and winter (Fig. 3d), the nucleation mode particles showed around 09:00 LT, a little bit later than spring and summer. The possible explanation is: the sun rises later than the other two seasons. The nucleation mode particles start to show at about 5 nm in fall and winter, a litter bit different from spring, 3 nm and summer, 10 nm, which is probably due to the meteorological factors which affect the NPF events as mentioned before.

The diurnal variation of the total particle number concentration and nucleation mode showed the same trend (Fig. 3e,f), which means the variation of the number concentration of nucleation mode particle takes a dominant role in the variation of total particle number concentration at SDZ. The nucleation mode particle concentration reached their peaks at different times due to the duration of NPF events (Fig. 3f). The highest number concentration of nucleation mode appeared in spring due to the most frequently NPF events and the lowest in summer which is because high temperature and high relative humidity, together with the stagnant air masses will cause the high condensation sink which prevents the NPF events (Wu et al., 2007). At SDZ, the mean temperature and relative humidity is 24 °C and 78%, respectively and the mean CS is 0.04 s^{-1} in summer which is two times as the mean CS during NPF events (0.02 s^{-1}). The lowest concentrations of Aitken mode particle occurred between 10:00–12:00 LT because of the clear air mass from aloft mixing downward as the development of boundary layer after sunrise, then increased due to condensational growth of nucleation mode particles, and remained stable all night till next morning until the mixing boundary layer changed next day (Fig. 3g). The lowest accumulation mode particle concentration was observed in the afternoon (Fig. 3h), which was mainly caused by the higher mixing layer. The diurnal variations of Aitken mode and accumulation mode particle concen-

ACPD
10, 25205–25242, 2010

tration at SDZ were different from those in the urban area of Beijing where the Aitken and accumulation mode had two or three peaks (around 08:00 and 20:00 LT), and the morning and night peaks were the result of traffic emissions (Wu et al., 2008).

For gaining insight into the seasonal variations of particle number size distribution, its parameterization in four seasons was discussed (Table 2). A least square fitting algorithm was used to parameterize the particle number size distributions by a multiple lognormal function (Birmili et al., 2001). The median number size distributions of particles below 1 µm were represented by three lognormal modes. Here, a least squares fitting algorithm was used to parameterize the particle number size distributions by a multiple lognormal function (Birmili et al., 2001). Three modes (i=1,2,3) were used corresponding to the nucleation mode, Aitken mode, and accumulation mode, respectively. The log-normal distribution is expressed as (Seinfeld and Pandis, 1998):

$$\frac{dN}{d\log D_p} = \sum_{i=1}^{n} \frac{N_i}{\sqrt{2\pi}\log\sigma_i} \exp\left(-\frac{\left(\log D_p - \log \overline{D}_{p,i}\right)^2}{2(\log\sigma_i)^2}\right) \quad (1)$$

where N_i is the total number concentration of the mode i, $\overline{D}_{p,i}$ is the geometric mean diameter of mode i, σ_i is the geometric mean standard deviation of the distribution and n is the number of the modes. In this study, log means always log10.

As shown in Table 2, fitted number concentrations of three modes, N_1, N_2, and N_3 were all higher in spring than those in the other seasons as a result of frequent NPF events with high formation rates (discussed in the following paragraph). The geometric mean diameter in summer was higher than those in other seasons. In summer, high condensable vapor concentration favored condensational growth of particles. Fall is a harvest time, so agricultural biomass burning might contribute to the accumulation mode particles. Li et al. (2007) showed that geometric mean diameters of particles emitted by all kinds of biofuels combustion were in the range from 110 nm to 200 nm. In addition, the larger geometric mean diameters of accumulation mode particles in summer and fall should be associated with polluted episodes, which are characterized

ACPD
10, 25205–25242, 2010

by high number concentrations in the accumulation mode particles (Wu et al., 2008). The parameterized geometric mean diameters of nucleation mode (16–20 nm) and the number concentrations of Aitken mode (10 100–12 400 cm^{-3}) were higher in urban Beijing (Wu et al., 2008) than those in this study, which could be explained to a larger extent by the vehicular traffic activities in the urban area. The geometric mean diameter of the accumulation mode in Beijing (117–148 nm) was much lower than that at SDZ (173–199 nm), which indicated the particles condensational growth during the air mass long-range transportation from the urban to the rural site.

3.3 Back trajectories analysis

Transport of air constituents from source regions to receptor locations can be qualitatively described by numerical back trajectories. To investigate the impact of meteorological transport on the particle number concentrations at SDZ, 72 h backward trajectories were calculated using the HYSPLIT 4 model (Hybrid Single-Particle Lagrangian Integrated Trajectory) (Draxler and Rolph, 2003). As a main limitation, standard back trajectories are one-dimensional and do, particularly, not take into account mixing between air masses at various heights. A simple grouping of various trajectory pathways can provide a more realistic representation of plume dispersion to categorize the source region (Verma et al., 2007). For SDZ, 3-D back trajectories were calculated four times for each day, 00:00, 06:00, 12:00 and 18:00 UTC, terminating in a height of 100 m above ground level. 2192 trajectories were calculated and used to do the air mass cluster analysis. In this work we applied a k-means cluster algorithm similar to that described in Engler et al. (2007). As a distance measure between individual trajectories, longitude and latitude (in degrees) as well as the height of the trajectory above the ground were considered for each hourly trajectory point. To reduce the overemphasis of trajectory points far away, the distance measure was weighted by a function that decreased linearly from the receptor point to the end of the 72 h-trajectory. To compare horizontal (degree) and vertical (meter) distances, several cluster algorithm runs were conducted using different weights for the vertical distance. Here, we present results for

ACPD
10, 25205–25242, 2010

the weighing factor that separated the clusters in terms of mean particle number size distributions best.

Figure 4 shows the mean back trajectories for three clusters. The three clusters represented 99% of the total back trajectories, i.e., cluster 1, 2, 3 accounted for 38%, 24% and 37%, respectively. As can be seen in Fig. 4, clusters mainly originate from two directions, northwesterly (cluster 1, 2) and southeasterly (cluster 3). The mean back trajectories showed significant differences in direction but also in length, and therefore represented the main classes of atmospheric flow conditions over Northeastern China. Cluster 1 from Mongolia passed over Inner Mongolia and Hebei province, cluster 2 from Russia passed over Mongolia, Inner Mongolia and Hebei province, while cluster 3 from Bohai passed over the North China Plain region. Cluster 1 and 2 were from high altitudes (above 1000 m) while cluster 3 was from lower altitudes (below 500 m). Air masses northwesterly originated were usually connected with the advection of dry and clean continental air into SDZ. Air mass from southeasterly direction moved slowly and spent much more time over the industrialized regions favoring accumulation of aerosol particles and condensational growth by vapors.

Figure 5 shows contour diagrams of the diurnal variation of number size distributions, averaged over all days (4 back trajectories a day) belonging to the same cluster that introduced above, i.e., 45 days for cluster 1, 40 days for cluster 2 and 95 days for cluster 3. Significant differences were recognizable: cluster 3 showed the highest number concentrations around a particle size of 100–200 nm. The geometric mean diameter in cluster 3 was relatively stable during the whole day which is consistent with a previous study in Beijing city. Wehner et al. (2008) applied trajectories clustering to analyze 3-year trajectories and their relation to particle number size distributions in Beijing city. They found that the air parcels, whose pathways was similar to cluster 3 of this study, had the highest concentration of PM_1 resulting from the uptake of anthropogenic pollution in the south of Beijing. In contrast, clusters with fast moving air masses from the northwest (clusters 1, 2) showed a clear nucleation in the late morning growing into the Aitken mode at noon indicating frequent NPF events. An explanation for the nucleation

ACPD
10, 25205–25242, 2010

process in the northerly air masses is its efficient vertical dilution and therefore a relatively low pre-existing particle surface area (Wehner et al., 2008).

The diurnally averaged time series of the total number and mass concentration are shown in Fig. 6. The general differences in particles number and mass concentration were also obvious: cluster 1 showed the highest number concentrations of particles during daytime from 08:00 to 16:00 LT, which was the period of NPF events (Fig. 6a). The mass concentration of cluster 3 was much higher than those of others (Fig. 6b), indicating the significant contribution of accumulation range particles from regional pollution sources south of the measurement site to the mass concentration. The analysis above revealed that air masses from northwest were associated with high number concentration of nucleation and Aitken mode particles, while air masses from southeast were associated with high accumulation mode particles concentration.

3.4 New particle formation events

The analysis of NPF events in this study consists of the identification of NPF bursts, obtaining characteristics like growth and formation rates of new particles and the condensational sink (CS). The identification of NPF events was based on the principles and methods presented in Dal Maso et al. (2005). A distinct new mode of particles (3–25 nm) had to appear in the size distribution in the nucleation mode and prevail for at least an hour. In addition, the new mode was required to increase in diameter during its detection. The formation and growth rates and other characteristics of the NPF events were also calculated following the treatment in Dal Maso et al. (2005). The size distributions were parameterized by a least-square log-normal fitting method yielding parameters of 2–3 log-normal modes. So, the time series of geometric mean diameter ($D_{p,g}$) of nucleation mode could be obtained, thus, the growth rate (GR=$dD_{p,g}/dt$, given in nm h^{-1}) was calculated. The observed change in new particle concentration (dN_{nuc}/dt) was defined as the temporal change of 3–25 nm particle concentration (N_{nuc}) between the start of particle appearance and the peak in N_{nuc}, according to Dal

ACPD
10, 25205–25242, 2010

Maso et al. (2007). The observed formation rate of new particles (J_{obs}) was calculated according to Eq. (2):

$$J_{obs} = \frac{dN_{nuc}}{d_t} + F_{coag} \quad (2)$$

where N_{nuc} is the nucleated particle concentration, F_{coag} is the loss of particles due to coagulation. F_{coag} can be calculated using Eq. (3):

$$F_{coag} = \mathrm{CoagS}_{nuc} N_{nuc} \quad (3)$$

where CoagS_{nuc} is the coagulation sink of particles in the nucleation mode. The reference size for CoagS_{nuc} is assumed to be the geometric mean diameter of the fitted nucleation mode. A mean value of F_{coag} over the observed formation period was taken.

CoagS_{nuc} is defined as

$$\mathrm{CoagS}(D_p) = \int K(D'_p, D_p) n(D'_p) dD'_p \quad (4)$$

while $K(D'_p, D_p)$ is the coagulation coefficient (kernel) of particles with sizes D_p and D'_p, calculated by using the formula of Fuchs (1964) .

CS describes the ability of the size distribution to remove condensable vapors from the atmosphere. In practice, the vapor is assumed to have a very low vapor pressure at the surface of the particle, and molecular properties similar to sulfuric acid (Dal Maso et al., 2005). The parameter CS is defined as

$$\mathrm{CS} = 2\pi D \sum \beta_m(D_{p,i}) D_{p,i} N_i \quad (5)$$

where $D_{p,i}$ is the diameter of a particle in size class i and N_i is the particle concentration in the respective size class. D is the diffusion coefficient of the condensing vapor. We used the transition regime correction factor β_m from Fuchs and Sutugin (1970).

During the measurement period, 181 NPF events were observed corresponding to 36% of the effective measurement days. Figure 7 shows the annual variation of NPF

ACPD
10, 25205–25242, 2010

event occurrence, indicating that NPF events occur more frequently in spring and winter and less frequent in summer. This variation is quite similar with the frequency of NPF events in Beijing between March 2004 and February 2005 (Wu et al., 2007).

The range of formation rate (J_{obs}) varied from 0.7–72.7 $cm^{-3}\,s^{-1}$, with the mean value 8 $cm^{-3}\,s^{-1}$, which was lower than the results observed at some urban sites, such as in Beijing, 3.3–81.4 $cm^{-3}\,s^{-1}$ (Wu et al., 2007), St. Louis, with the mean value 17 $cm^{-3}\,s^{-1}$ (Qian et al., 2007), but much higher than those at some rural sites, such as Hyytiälä, Finland, 0.7 $cm^{-3}\,s^{-1}$, Melpitz, Germany, 4.6 $cm^{-3}\,s^{-1}$ and San Pietro Capofiume, Italy, 3.6 $cm^{-3}\,s^{-1}$ (Jaatinen et al., 2009). Whatever, the formation rate at SDZ is comparable with the results observed in boundary layer regional nucleation events 0.01–10 $cm^{-3}\,s^{-1}$ at most other sites (Kulmala et al., 2004). The contribution of the coagulation loss flux F_{coag} was on average 40% of the total observed rate, which was quite close to the average ratio of coagulation loss to formation rate observed in Beijing, 0.41 (Yue et al., 2010), meaning coagulation loss was the same important as the net rate of increase of nucleation mode particles (dN_{nuc}/dt). The growth rate (GR) ranged from 0.3 to 14.5 $nm\,h^{-1}$, with the mean value 4.3 $nm\,h^{-1}$, close to the growth rate in Beijing 0.3–11.2 $nm\,h^{-1}$ (Wu et al., 2007) and also in the range of typical particle growth rates 1–20 $nm\,h^{-1}$ in mid-latitudes (Kulmala et al., 2004), but higher than that at Hyytiälä, 2.9 $nm\,h^{-1}$ (Jaatinen et al., 2009), and lower than that at some sites, such as Melpitz, 6.2 $nm\,h^{-1}$, San Pietro Capofiume 6.1 $nm\,h^{-1}$ (Jaatinen et al., 2009) and St. Louis, 5.9 $nm\,h^{-1}$ (Qian et al., 2007). The annual variations of formation and growth rates are shown in Fig. 8, indicating that the formation rate was higher in spring while the growth rate was higher in summer. An explanation for this observation is the meteorological condition, e.g. solar radiance, low temperature and humidity and low CS favoring the new particle formation in spring. In summertime the enhancement of photochemical and biological activities together with the stagnant air masses preventing exchange with cleaner air contributed to the particle growth caused by condensation of low volatile vapors which resulted in higher CS then other seasons and prevented NPF to be observed. During NPF events CS was usually low, varying from 0.001 to 0.12 s^{-1}

ACPD
10, 25205–25242, 2010

with mean value of 0.02 s^{-1}.

3.5 The effects of new particle formation events: a case study

In the following, we focus on 13 March 2008, which is a typical new particle formation event. That means new particles are formed by nucleation in the morning followed by a clear condensation growth to accumulation mode indicated by the "banana-shaped" temporal development of the number size distribution (Fig. 9a). For this event, the J_{obs} is 14.9 cm^{-3} s^{-1} and GR is 3.8 nm h^{-1}. In Fig. 9b, the number concentrations of newly formed particles, 3–15 nm, the larger particles, 15–80 nm and the "aged" particles, 80–850 nm were calculated, respectively. Nucleation started at about 8:00, accompanied by the number concentration of 3–15 nm particles increased sharply to about 70 000 cm^{-3}. Then the newly formed particles grew to lager sizes, so the number concentrations of 15–80 nm and 80–850 nm particles increased with a few hours time lag. The wind direction was northeast and west dominated, which corresponded to the clean air mass. Nucleated particles, which grow up to 50–100 nm, can principally act as cloud condensation nuclei (CCN) (Kerminen et al., 2005). Here, the number concentration of particle in the range of 80–850 nm was calculated as the number concentration of potential CCN. The newly formed particles grew into the CCN size range when the number concentration of 80–850 nm particles increased rapidly after 20:00 LT. The mean formation rate was about 0.78 cm^{-3} s^{-1}, indicating that new particle formation events contributed significantly to the number concentration of CCN. The result of CAREBeijing-2006 also revealed that the nucleation mode grew very quickly into the size range of CCN, and the CCN size distribution was dominated by the growing nucleation mode (Wiedensohler et al., 2009).

Furthermore, new particles can grow to larger sizes (>100 nm) affecting also the optical properties of the atmospheric particles (Allan et al., 2006). The refractive index is dependent on the two components, elemental carbon (EC) and non-light-absorbing species. The dry aerosol extinction coefficients were reconstructed with

ACPD
10, 25205–25242, 2010

extreme external and internal mixing of these two components (Cheng et al., 2006) utilizing a Mie code (Bohren et al., 1998), to derive the bounding values for the real mixing state. The mass concentration of EC was assumed to be constant at 2.12 $\mu g\,m^{-3}$ which was the mean daily-average concentration during nearly two years measurement at SDZ (Yan et al., 2008). The density of BC was taken as 1.5 $g\,cm^{-3}$. The refractive index used for non-light-absorbing component was 1.55–10^{-7} *i* (Sloane et al., 1984) and the refractive index of EC was 1.80–0.54 *i* (d'Almeida et al., 1991). The result (not shown here) indicated that the effect of two different mixing states on the extinction coefficient was less than 10%, and the average of the bounding values was used as the real extinction coefficient $\sigma_{ext,550nm}$. As shown in Fig. 9c, $\sigma_{ext,550nm}$ increased at the rate of 49 $Mm^{-1}\,h^{-1}$ from 20:30 LT to the end of day.

The PM_1 mass concentration was calculated using measured number size distribution (mobility diameter less than 1 µm) with assumed density of 1.7 $g\,cm^{-3}$. The PM_1 mass showed a significant increase from 20:30 to 24:00 LT with the average growth rate 18 $\mu g\,m^{-3}\,h^{-1}$ (see Fig. 9c), which is consistent with the previous results at Yufa site, a rural site south of Beijing (Wiedensohler et al., 2009).

In order to exclude possible physical effects such as evolution of boundary layer and advection, the concentration of CO was used for normalizing the particle number concentration, mass concentration and extinction coefficient (Su et al., 2008). As seen in Fig. 9d, the normalized number concentration of particles in the range of 80–850 nm increased by 450% from 20:00 LT to the end of the day, and the normalized PM_1 mass concentration and $\sigma_{ext,550nm}$ increased by 160% and 178% from 20:30 to 24:00 LT, respectively. The analysis above indicates that condensational growth of nucleated particles leads to an increase in the number concentration of potential CCN, aerosol mass concentration, and extinction coefficient, through which affect the climate and air quality.

All NPF events were selected to obtain mean diurnal particle size distributions and mass concentrations for the different seasons, as shown in Fig. 10. The particle mean diameter of the dominating mode (Peak diameter) was derived by mode fitting of the

ACPD
10, 25205–25242, 2010

mean diurnal particle size distributions. The mean growth rates of the nucleation mode for spring, summer, fall, and winter are 3.0, 4.2, 3.1 and 3.7 nm h^{-1}, respectively. The highest particle diameter growth rate appeared in summer because of the high condensable vapor concentration. The plots above showed a nearly linear increase in PM_1 mass concentrations and the particle mean diameter emphasized the mass contribution and the particle growth as a result of NPF events. The mean PM_1 mass growth rates for the four seasons are 2.1, 2.3, 4.1 and 5.3 µg m^{-3} h^{-1} during the time period from noon to the end of the day. The growth rates in fall and winter were much higher. There is however no clear explanation for this mass growth rate.

4 Conclusions

One and a half years continuous measurements were conducted at a rural site, Shangdianzi (SDZ), from March 2008 to August 2009, with the equipment of TDMPS and APS. The measurements covered the size range from 3 nm to 10 µm. This was the first long-term investigation of particle number size distributions at a regional background site in the North China Plain. It provided new insights into the evolution of particle number size distribution and new particle formation events for testing and validating regional and global climate models.

During the measurement, the number concentration of nucleation mode, Aitken mode, accumulation mode and total particles were $3.6\pm7.9\times10^3$ cm^{-3}, $4.4\pm3.4\times10^3$ cm^{-3}, $3.5\pm2.8\times10^3$ cm^{-3} and $1.2\pm0.9\times10^4$ cm^{-3}, respectively. The number concentration at SDZ had a significant seasonal variation. The peak of the total particle number concentration appeared in spring due to the frequent new particle formation events and the minimum in summer. The diurnal variation of particle number concentration was also influenced by new particle formation events. The nucleation mode particle bursts caused also peaks in total particle number concentrations and later also Aitken mode particles reached their maximum as a result of newly formed particle condensational growth.

ACPD
10, 25205–25242, 2010

Back trajectories analysis revealed that air masses arriving at SDZ mainly originated from northwest and southeast. Polluted air masses from urban areas of Beijing, and even some polluted areas in south of Beijing at North China Plain, could be easily transported to SDZ along with the southeasterly origin, while relatively clean air masses were transported to SDZ mainly from northwest. In summer, the southeasterly air mass dominated, while in other seasons the northwesterly air mass dominated. On average, the number concentration of nucleation mode particles was much higher in air masses from northwestern clean areas which favored the new particle formation events. Air masses from southeast were usually related to high number concentration of accumulation mode particles because they were slow-moving and vertically stable could favors the accumulation of anthropogenic emissions mainly from North China Plain. In this situation, the condensational sink of pre-existing particles were high that inhabited the new particle formation events. The cluster analysis at SDZ was quite similar to that in Beijing.

New particle formation events occurred quite frequently at SDZ, amounting to 36% of all the effective measurement days. The range of formation rate varied from 0.7 to 72.7 $cm^{-3}\,s^{-1}$, and the coagulation loss part contributed to about 40%. The growth rate ranged from 0.3 to 14.5 $nm\,h^{-1}$, and in most cases, the condensational growth of newly formed particles contributes to particle sizes which have the potential to act as CCN, increase the aerosol mass concentration and extinction coefficient.

Acknowledgements. This work was supported by European Integrated project on Aerosol Cloud Climate and Air Quality Interactions, EUCAARI (036833), The China International Science and Technology Cooperation Project (2009DFA22800), the National Natural Science Foundation of China (40575063), National Basic Research Program of China (2006CB403703, 2006CB403701). The authors are highly appreciated that Xu Xiaobin and Lin Weilin provided the reactive gas data, and also thank the Shangdianzi staff for operating and maintaining the instruments at the station.

ACPD
10, 25205–25242, 2010

References

Allan, J. D., Alfarra, M. R., Bower, K. N., Coe, H., Jayne, J. T., Worsnop, D. R., Aalto, P. P., Kulmala, M., Hyötyläinen, T., Cavalli, F., and Laaksonen, A.: Size and composition measurements of background aerosol and new particle growth in a Finnish forest during QUEST 2 using an Aerodyne Aerosol Mass Spectrometer, Atmos. Chem. Phys., 6, 315–327, doi:10.5194/acp-6-315-2006, 2006.

Barsanti, K. C., McMurry, P. H., and Smith, J. N.: The potential contribution of organic salts to new particle growth, Atmos. Chem. Phys., 9, 2949–2957, doi:10.5194/acp-9-2949-2009, 2009.

Birmili, W., Stratmann, F., and Wiedensohler, A.: Design of a DMA-based size spectrometer for a large particle size range and stable operation, J. Aerosol Sci., 30 (4), 549–554, 1999.

Birmili, W., Wiedensohler, A., Heintzenberg, J., and Lehmann, K.: Atmospheric particle number size distribution in Central Europe: statistical relations to air mass and meteorology, J. Geophys. Res., 32, 5–18, 2001.

Bohren, C. F. and Huffman, D. R.: Absorption and Scattering of Light by Small Particles, John Wiley and Sons, New York, 1998.

Boy, M. and Kulmala, M.: Nucleation events in the continental boundary layer: Influence of physical and meteorological parameters, Atmos. Chem. Phys., 2, 1–16, doi:10.5194/acp-2-1-2002, 2002.

Boy, M., Kulmala, M., Ruuskanen, T. M., Pihlatie, M., Reissell, A., Aalto, P. P., Keronen, P., Dal Maso, M., Hellen, H., Hakola, H., Jansson, R., Hanke, M., and Arnold, F.: Sulphuric acid closure and contribution to nucleation mode particle growth, Atmos. Chem. Phys., 5, 863–878, doi:10.5194/acp-5-863-2005, 2005.

Cheng, Y. F., Eichler, H., Wiedensohler, A., Heintzenberg, J., Zhang, Y. H., Hu, M., Herrmann, H., Zeng, L. M., Liu, S., Gnauk, T., Brüggemann, E., and He, L. Y.: Mixing state of elemental carbon and non-light-absorbing aerosol components derived from in situ particle optical properties at Xinken in Pearl River Delta of China, J. Geophys. Res., 111, D20204, doi:10.1029/2005JD006929, 2006.

Dal Maso, M., Kulmala, M., Riipinen, I., Wagner, R., Hussein, T., Aalto, P. P., and Lehtinen, K. E. J.: Formation and growth of fresh atmospheric aerosols: eight years of aerosol size distribution data from SMEAR II, Hyytiälä, Finland, Boreal Environ. Res., 10, 323–336, 2005.

ACPD
10, 25205–25242, 2010

Dal Maso, M., Sogacheva, L., Aalto, P. P., Riipinen, I., Komppula, M., Tunved, P., Korhonen, L., Suur-Uski, V., Hirsikko, A., Kurten, T., Kerminen, V.-M., Lihavainen, H., Viisanen, Y., Hansson, H.-C., and Kulmala, M.: Aerosol size distribution measurements at four Nordic field stations: identification, analysis and trajectory analysis of new particle formation bursts, Tellus, 59, 350–361, 2007.

d'Almeida, G., Keopke, P., and Shettle, E.: Atmospheric Aerosol-Global Climatology and Radiative Characteristics, A. Deepak, Hampton, VA, 1991.

Dominici, F., Peng, R. D., Bell, M. L., Pham, L., McDermott, A., Zeger, S. L., and Samet, J. M.: Fine particulate air pollution and hospital admission for cardiovascular and respiratory diseases, J. Amer. Med. Assoc., 295, 1127–1134, 2006.

Draxler, R. R. and Rolph, G. D.: HYSPLIT (HYbrid Single-Particle Lagrangian Integrated Trajectory), model access via NOAA ARL READY Website at: http://www.arl.noaa.gov/ready/hysplit4.html, NOAA Air Resources Laboratory, Silver Spring, MD, 2003.

Engler, C., Rose, D., Wehner, B., Wiedensohler, A., Brüggemann, E., Gnauk, T., Spindler, G., Tuch, T., and Birmili, W.: Size distributions of non-volatile particle residuals (D_p<800nm) at a rural site in Germany and relation to air mass origin, Atmos. Chem. Phys., 7, 5785–5802, doi:10.5194/acp-7-5785-2007, 2007.

Fuchs, N. A.: The Mechanics of Aerosols, Pergamon, New York, 1964.

Fuchs, N. A. and Sutugin, A. G.: Highly Dispersed Aerosols, Pergamon, New York, 1971.

Gao, J., Wang, J., Cheng, S. H., Xue, L. K., Yan, H. Z., Hou, L. J., Jiang, Y. Q., and Wang, W. X.: Number concentration and size distributions of submicron particles in Jinan urban area: characteristics in summer and winter, J. Environ. Sci., 19, 1466–1473, 2007.

Gao, J., Wang, T., Zhou, X. H., Wu, W. S., and Wang, W. X.: Measurement of aerosol number size distributions in the Yangtze River Delta in China: formation and growth of particles under polluted conditions, Atmos. Environ., 43, 829–836, 2009.

Harrison, R. M., Jones, M., and Collins, G.: Measurements of the physical properties of particles in the urban atmosphere, Atmos. Environ., 33, 309–321, 1999.

Hamed, A., Joutsensaari, J., Mikkonen, S., Sogacheva, L., Dal Maso, M., Kulmala, M., Cavalli, F., Fuzzi, S., Facchini, M. C., Decesari, S., Mircea, M., Lehtinen, K. E. J., and Laaksonen, A.: Nucleation and growth of new particles in Po Valley, Italy, Atmos. Chem. Phys., 7, 355–376, doi:10.5194/acp-7-355-2007, 2007.

Hong, Y. C., Lee, J. T., Kim, H., Ha, E. H., Schwartz, J., and Christiani, D. C.: Effects of air pollutants on acute stroke mortality, Environ. Health Persp., 110, 181–197, 2002.

ACPD
10, 25205–25242, 2010

Hussein, T., Puustinen, A., Aalto, P. P., Mäkelä, J. M., Hämeri, K., and Kulmala, M.: Urban aerosol number size distributions, Atmos. Chem. Phys., 4, 391–411, doi:10.5194/acp-4-391-2004, 2004.

Intergovernmental Panel on Climate Change (IPCC): Intergovernmental Panel on Climate Change (IPCC): Summary for policymakers, Climate Change 2007: The Physical Science Basis, edited by: Solomon, S., Qin, D. H., Manning, M., Marquis, M., Averyt, K., Tignor, M., Miller, H. L., and Chen, Z. L., Cambridge University Press, Cambridge, 2007.

Iida, K., Stolzenburg, M. R., and McMurry, P. H.: Effect of working fluid on sub-2 nm particle detection with a laminar flow ultrafine condensation particle counter, Aerosol Sci. Tech., 43, 81–96, doi:10.1080/02786820802488194, 2008.

Jaatinen, A., Hamed, A., Joutsensaari, J., Mikkonen, S., Birmili, W., Wehner, B., Spindler, G., Wiedensohler, A., Decesari, S., Mircea. M., Facchini. M. C., Junninen, H., Kulmala, M., Lehtinen, K. E. J., and Laaksonen, A.: A comparison of new particle formation events in the boundary layer at three different sites in Europe, Boreal Env. Res., 14, 481–498, 2009.

Kerminen, V.-M., Lihavainen, H., Komppula, M., Viisanen, Y. and Kulmala, M.: Direct observational evidence linking atmospheric aerosol formation and cloud droplet activation, Geophys. Res. Lett., 32, L14803, doi:10.1029/2005GL023130, 2005.

Kerminen, V.-M. and Kulmala, M.: Analytical formulae connecting the "real" and the "apparent" nucleation rate and the nuclei number concentration for atmospheric nucleation events, J. Aerosol Sci., 33, 609–622, 2002.

Kivekäs, N., Sun, J., Zhan, M., Kerminen, V.-M., Hyvärinen, A., Komppula, M., Viisanen, Y., Hong, N., Zhang, Y., Kulmala, M., Zhang, X.-C., Deli-Geer, and Lihavainen, H.: Long term particle size distribution measurements at Mount Waliguan, a high-altitude site in inland China, Atmos. Chem. Phys., 9, 5461–5474, doi:10.5194/acp-9-5461-2009, 2009.

Kulmala, M.: How particles nucleate and grow, Science, 302, 1000–1001, 2003.

Kulmala, M., Vehkamäkia, H., Petäjä, T., Dal Maso, M., Lauri, A., Kerminen, V.-M., Birmili, W., and McMurry, P. H.: Formation and growth rates of ultrafine atmospheric particles: a review of observations, J. Aerosol Sci., 35, 143–176, 2004.

Kulmala, M., Riipinen, I., Sipilä, M., Manninen, H. E., Petäjä, T., Junninen, H., Dal Maso, M., Mordas, G., Mirme, A., Vana, M., Hirsikko, A., Laakso, L., Harrison, R. M., Hanson, I., Leung, C., Lehtinen, K. E. J., and Kerminen, V. -M.: Toward direct measurement of atmospheric nucleation, Science, 318, 89–92, 2007

Laakso, L., Koponen, I. K., Mönkkönen, P., Kulmala, M., Kerminen, V.-M., Wehner, B., Wieden-

ACPD
10, 25205–25242, 2010

sohler, A., Wu, Z. J., and Hu, M.: Aerosol particles in the developing world: a comparison between New Delhi in India and Beijing in China, Water Air Soil Poll., 173, 5–20, 2006.
Li, X. H., Duan, L., Wang, S. X., Duan, J. C., Guo, X. M., Yi, H. H., Hu, J. N., Li, C., and Hao, J. M.: Emission characteristics of particulate matter from rural household biofuel combustion in China, Energ. Fuel., 21, 845–851, 2007.
Liu, S., Hu, M., Wu, Z. J., Wehner, B., Wiedensohler, A., and Cheng, Y. F.: Aerosol number size distribution and new particle formation at a rural/coastal site in Pearl River Delta (PRD) of China, Atmos. Environ., 25, 6275–6283, 2008.
Middleton, W. E. K.: Vision Through the Atmosphere, University of Toronto Press, Toronto, 1952.
Pope III., C. A. and Dockery, D. W.: Health effects of fine particulate air pollution: lines that connect, J. Air Waste Manage., 56, 709–742, 2006.
Riipinen, I., Sihto, S.-L., Kulmala, M., Arnold, F., Dal Maso, M., Birmili, W., Saarnio, K., Teinilä, K., Kerminen, V.-M., Laaksonen, A., and Lehtinen, K. E. J.: Connections between atmospheric sulphuric acid and new particle formation during QUEST III–IV campaigns in Heidelberg and Hyytiälä, Atmos. Chem. Phys., 7, 1899–1914, doi:10.5194/acp-7-1899-2007, 2007.
Rosenfeld, D., Lohmann,U., Raga, G. B., O'Dowd, C. D., Kulmala, M., Fuzzi, S., Reissell, A., and Andreae, M. O.: Flood or drought: how do aerosols affect precipitation?, Science, 321, 1309–1313, 2008.
Seinfeld, J. H. and Pandis, S. N.: Atmospheric Chemistry and Physics of Air Pollution, John Wiley and Sons, Inc., New York, 1998.
Qian, S., Sakurai, H., and McMurry, P. H.: Characteristics of regional nucleation events in urban East St. Louis, Atmos. Environ., 41, 4119–4127, 2007.
Sloane, C. S.: Optical properties of aerosols of mixed composition, Atmos. Environ., 18, 871–878, 1984.
Stanier, C. O., Khlystov, A. Y., and Pandis, S. N.: Ambient aerosol size distributions and number concentrations measured during the Pittsburgh Air Quality Study (PAQS), Atmos. Environ., 38, 3275–3284, 2004.
Su, H., Cheng, Y. F., Cheng, P., Zhang, Y. H., Dong, S. F., Zeng, L. M., Wang, X. S., Slanina, J., Shao, M., and Wiedensohler, A.: Observation of nighttime nitrous acid (HONO) formation at a non-urban site during PRIDE-PRD 2004 in China, Atmos. Environ., 42, 6219–6232, 2008.
Sipilä, M., Lehtipalo, K., Attoui, M., Neitola, K., Petäjä, T., Aalto, P. P., O'Dowd, C. D., and

ACPD
10, 25205–25242, 2010

Kulmala, M.: Laboratory verification of PH-CPC's ability to monitor atmospheric sub-3 nm clusters, Aerosol Sci. Tech., 43, 126–135, 2009.
Twomey, S.: Atmospheric Aerosols, Elsevier, New York, 1977.
Tuch, T. M., Haudek, A., Müller, T., Nowak, A., Wex, H., and Wiedensohler, A.: Design and performance of an automatic regenerating adsorption aerosol dryer for continuous operation at monitoring sites, Atmos. Meas. Tech., 2, 417–422, doi:10.5194/amt-2-417-2009, 2009.
Verma, S., Venkataraman, C., Boucher, O., and Ramachandran, S.: Source evaluation of aerosols measured during the Indian Ocean Experiment using combined chemical transport and back trajectory modeling, J. Geophys. Res., 112, D11210, doi:10.1029/2006JD007698, 2007.
Wang, W., Ma, J. Z., Hatakeyama, S., Liu, X. Y., Chen, Y., Takami, A., Ren, L. H., and Geng, C. M.: Aircraft measurements of vertical ultrafine particles profiles over Northern China coastal areas during dust storms in 2006, Atmos. Environ., 42, 5715–5720, 2008.
Wehner, B., Birmili, W., Ditas, F., Wu, Z., Hu, M., Liu, X., Mao, J., Sugimoto, N., and Wiedensohler, A.: Relationships between submicrometer particulate air pollution and air mass history in Beijing, China, 2004–2006, Atmos. Chem. Phys., 8, 6155–6168, doi:10.5194/acp-8-6155-2008, 2008.
Wehner, B. and Wiedensohler, A.: Long term measurements of submicrometer urban aerosols: statistical analysis for correlations with meteorological conditions and trace gases, Atmos. Chem. Phys., 3, 867–879, doi:10.5194/acp-3-867-2003, 2003.
Wiedensohler, A., Cheng, Y. F., Nowak, A., Wehner, B., Achtert, P., Berghof, M., Birmili, W., Wu, Z. J., Hu, M., Zhu, T., Takegawa, N., Kita, K., Kondo, Y., Lou, S. R., Hofzumahaus, A., Holland, F., Wahner, A., Gunthe, S. S., Rose, D., Su, H., and Pöschl, U.: Rapid aerosol particle growth and increase of cloud condensation nucleus activity by secondary aerosol formation and condensation: a case study for regional air pollution in Northeastern China, J. Geophys. Res., 114, D00G08, doi:10.1029/2008JD010884,2009.
Willeke, K. and Baron, P. A.: Aerosol Measurement: Principles, Techniques and Applications, Van Nostrand Reinhold, New York, 1993.
Woo, K. S., Chen, D. R., Pui, D. Y. H., and McMurry, P. H.: Measurement of Atlanta aerosol size distributions: observations of ultrafine particle events, Aerosol Sci. Tech., 34, 75–87, 2001.
Wu, Z. J., Hu, M., Liu, S., Wehner, B., Bauer, S., Maßling, A., Wiedensohler, A., Petäjä, T., Dal Maso, M., and Kulmala, M.: New particle formation in Beijing, China: Statistical analysis of a 1-year data set, J. Geophys. Res., 112, D09209, doi:10.1029/2006JD007406, 2007.

ACPD
10, 25205–25242, 2010

Wu, Z. J., Hu, M., Lin, P., Liu, S., Wehner, B., and Wiedensohler, A.: Particle number size distribution in the urban atmosphere of Beijing, China, Atmos. Environ., 42, 7967–7980, 2008.

Yan, P., Tang, J., Huang, J., Mao, J. T., Zhou, X. J., Liu, Q., Wang, Z. F., and Zhou, H. G.: The measurement of aerosol optical properties at a rural site in Northern China, Atmos. Chem. Phys., 8, 2229–2242, doi:10.5194/acp-8-2229-2008, 2008.

Yue, D. L., Hu, M., Wu, Z. J., Wang, Z. B., Guo, S., Wehner, B., Nowak, A., Achtert, P., Wiedensohler, A., Jung, J. S., Kim,Y. J., and Liu, S. H.: Characteristics of aerosol size distributions and new particle formation in the summer in Beijing, J. Geophys. Res., 114, D00G12, doi:10.1029/2008JD010894, 2009.

Yue, D. L., Hu, M., Zhang, R. Y., Wang, Z. B., Zheng, J., Wu, Z. J., Wiedensohler, A., He, L. Y., Huang, X. F., and Zhu, T.: The roles of sulfuric acid in new particle formation and growth in the mega-city of Beijing, Atmos. Chem. Phys., 10, 4953–4960, doi:10.5194/acp-10-4953-2010, 2010.

Zhang, R., Suh, I., Zhao, J., Zhang, D., Fortner, E. C., Tie, X., Molina, L. T., and Molina, M. J.: Atmospheric new particle formation enhanced by organic acids, Science, 304, 1487–1490, 2004.

ACPD
10, 25205–25242, 2010

Table 1. Overview of experimentally determined particle number concentrations in the troposphere over China.

	Number concentration (cm^{-3})				Reference
Diameter range (nm)	3–20	20–100	100–1000	3–10 000	Wu et al. (2008)
Beijing, urban	9000	15 900	7800	32 800	
Diameter range (nm)		10–100	100–500	10–500	Gao et al. (2007)
Jinan, urban summer, 2006		10 300	385	10 685	
winter, 2006		15 591	1796	17 387	
Diameter range (nm)		10–100	100–500	10–500	Gao et al. (2009)
Shanghai, suburban		28 511	1676	30 187	
Diameter range (nm)	3–20	20–100	100–1000	3–10 000	Yue et al. (2008)
Yufa, rural	2000	9000	5000	17 000	
Diameter range (nm)				3–10 000	Liu et al. (2008)
Xinken, rural/coastal				16 300	
Diameter range (nm)	12–21	21–95	95–570	12–570	Kivekäs et al. (2009)
Waliguan, remote rural	570	1060	430	2030	
Diameter range (nm)	3–25	25–100	100–1000	3–10 000	This work
Shangdianzi, rural	3610	4430	3470	11 510	

ACPD
10, 25205–25242, 2010

Table 2. Parameterization of Particle Number Size distribution for four seasons. The $\overline{D}_{p,i}$, σ_i and N_i represent the geometric mean diameter, geometric standard deviation and mean number concentration. Here i=1,2,3 corresponds to nucleation mode, Aitken mode and accumulation mode, respectively.

	N_1	σ_1	$\overline{D}_{p,1}$	N_2	σ_2	$\overline{D}_{p,2}$	N_3	σ_3	$\overline{D}_{p,3}$
Spring	19 100	2.33	12	9530	2.19	52	6630	1.66	181
Summer	3120	1.61	14	7420	2.05	61	4060	1.68	199
Fall	12 570	1.75	12	7660	2.13	58	3960	1.63	188
Winter	12 710	1.65	12	6550	2.07	52	5610	1.68	173

ACPD
10, 25205–25242, 2010

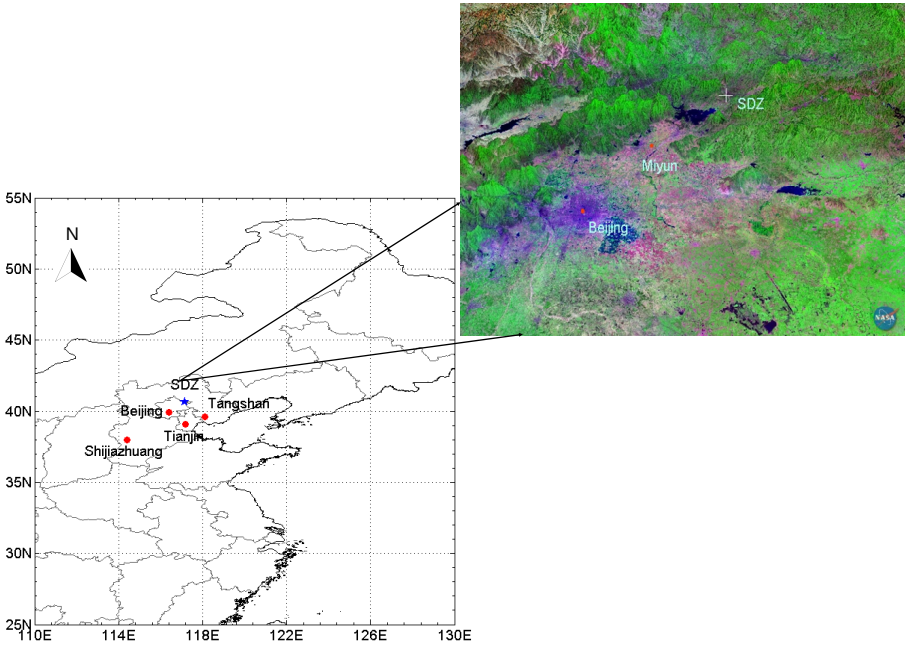

Fig. 1. Location of the SDZ station (blue star) and the main cities in Northern China (red dots) in the lower left panel. The upper right panel showing the topography and land use in the surrounding area, white cross indicating SDZ station, red dots indicating Minyun county and Beijing, respectively. NLT landsat7 pseudo color map is from http://worldwind.arc.nasa.gov. Vertical exaggeration is by a factor of 3.

ACPD
10, 25205–25242, 2010

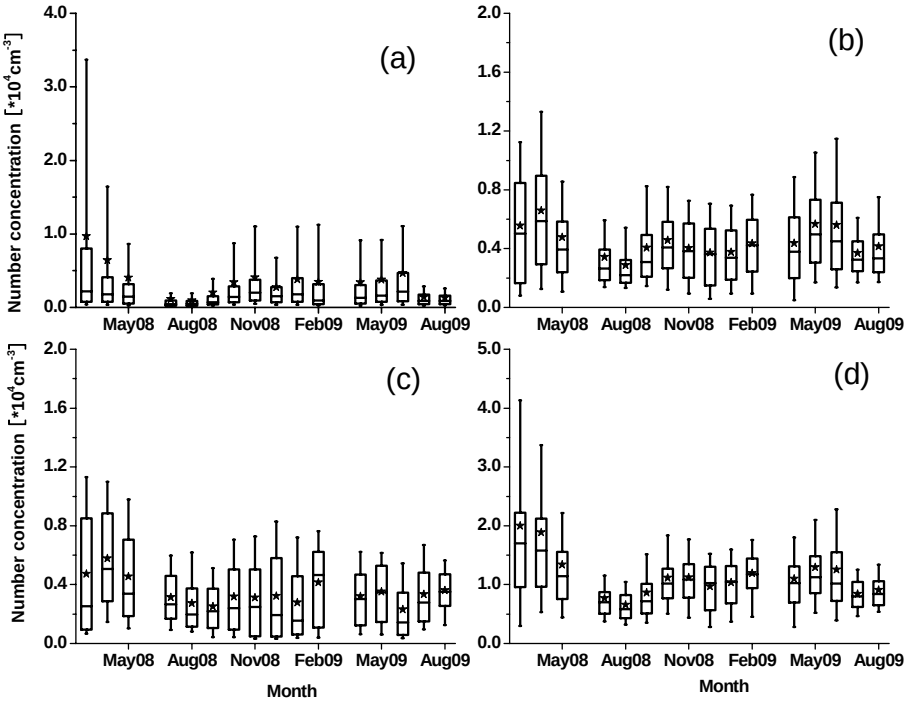

Fig. 2. Monthly variation of values for nucleation mode **(a)**, Aitken mode **(b)**, accumulation mode particles **(c)** and total particles **(d)** at SDZ. The box plots are read as follows: the upper and lower boundaries of the box indicate the 75th and the 25th percentiles, the line within the box marks the median, and the whiskers above and below the box indicate the 90th and 10th percentiles. The stars represent the mean values. There was no data available for June 2008 and March 2009.

ACPD
10, 25205–25242, 2010

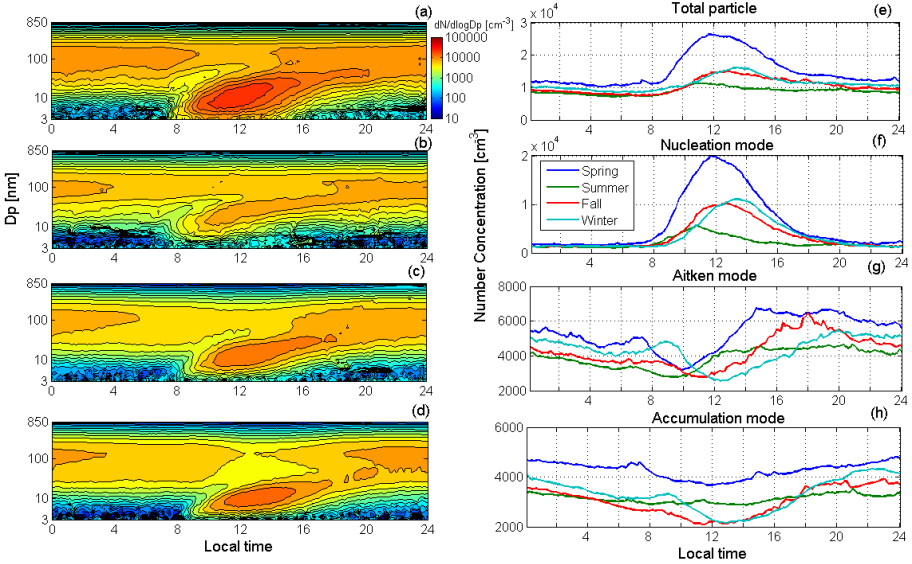

Fig. 3. Mean diurnal variations of the particle number size distributions **(a–d)** and seasonally diurnal variation of particle number concentrations in different modes **(e–h)**.

ACPD
10, 25205–25242, 2010

First long-term study of particle number size distributions

X. Shen et al.

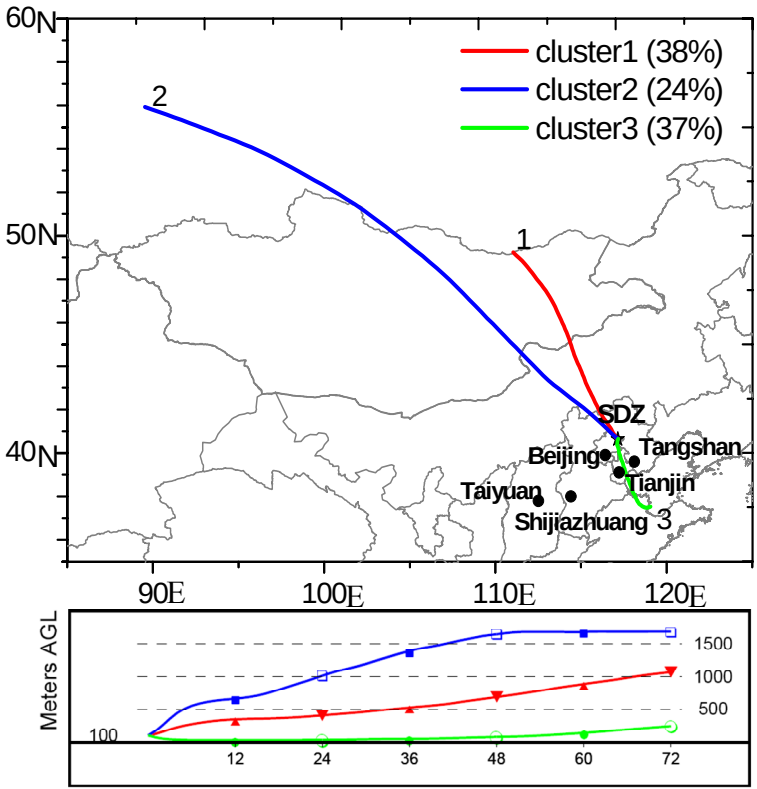

Fig. 4. Mean back trajectories for 3 trajectory clusters arriving at SDZ from different height, dots indicating the main cities of North China Plain.

ACPD
10, 25205–25242, 2010

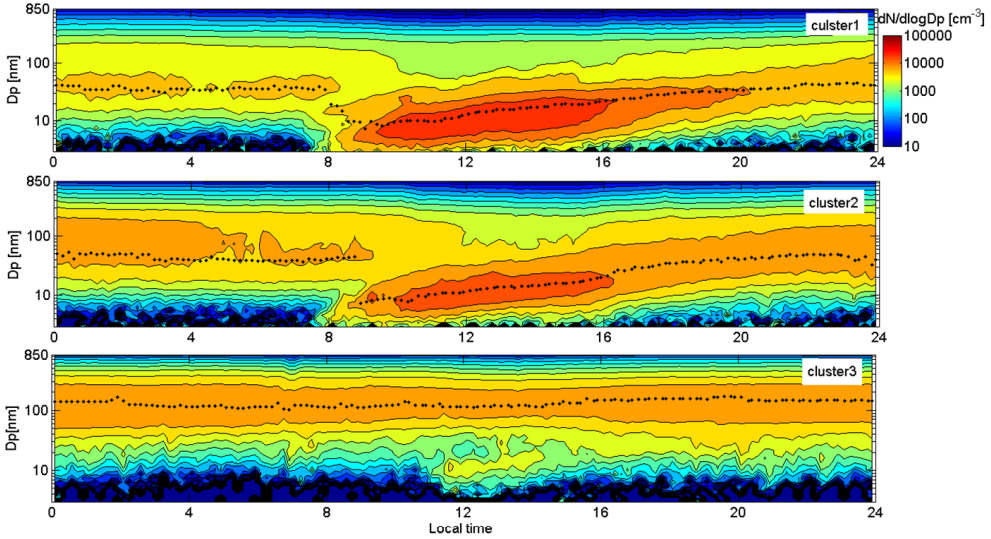

Fig. 5. Mean diurnal evolution of the particle number size distributions, averaged over the three trajectory clusters. Black dots indicate the mean diameter of the dominating mode.

ACPD
10, 25205–25242, 2010

First long-term study of particle number size distributions

X. Shen et al.

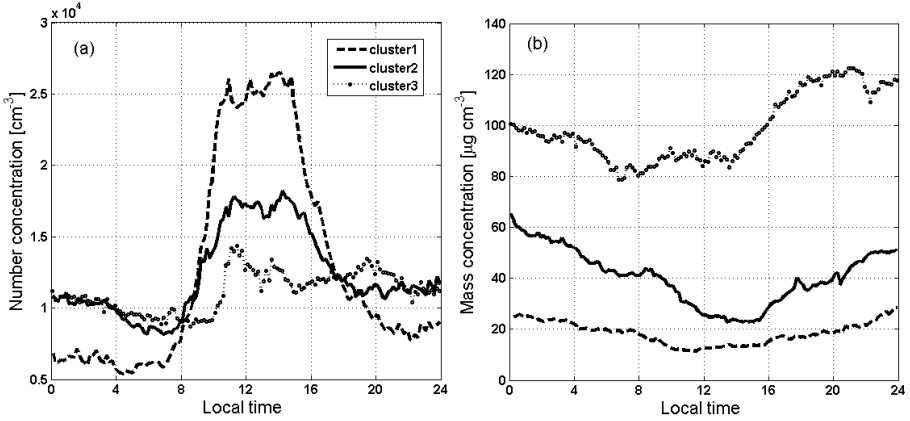

Fig. 6. Diurnal variation of total number concentration **(a)** and mass concentration **(b)** averaged over all days belonging to the same cluster.

ACPD
10, 25205–25242, 2010

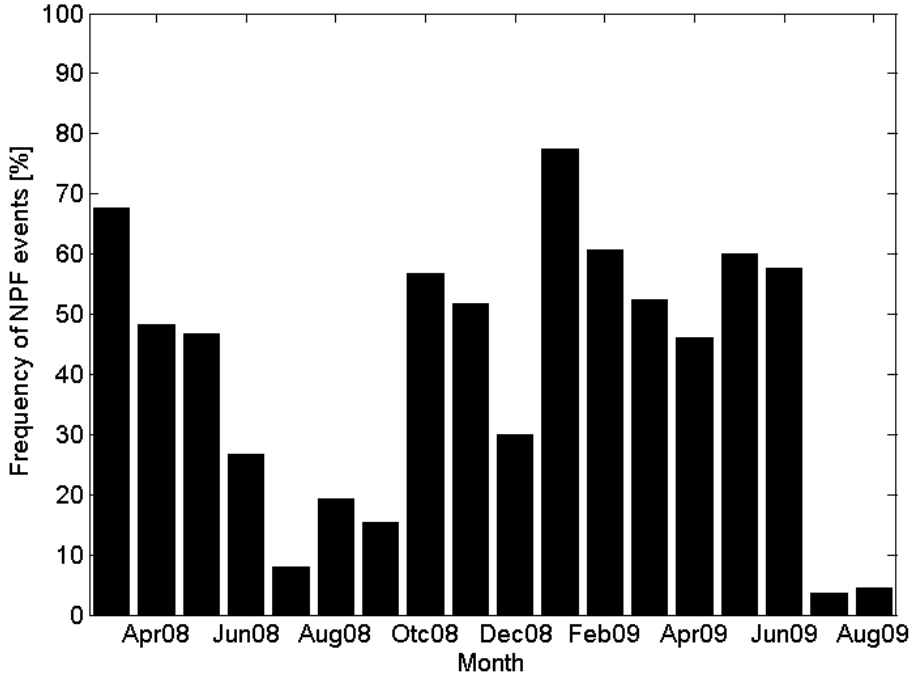

Fig. 7. Frequency of NPF events during each month.

ACPD
10, 25205–25242, 2010

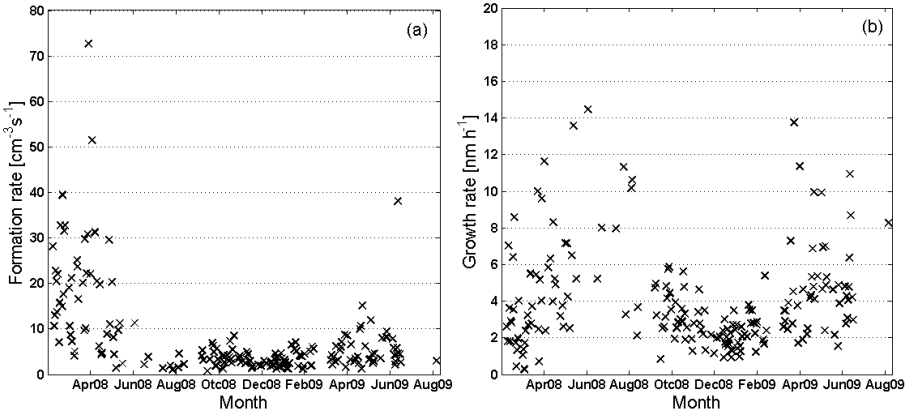

Fig. 8. The variation of formation rate **(a)** and growth rate **(b)** during measurement.

ACPD
10, 25205–25242, 2010

First long-term study of particle number size distributions

X. Shen et al.

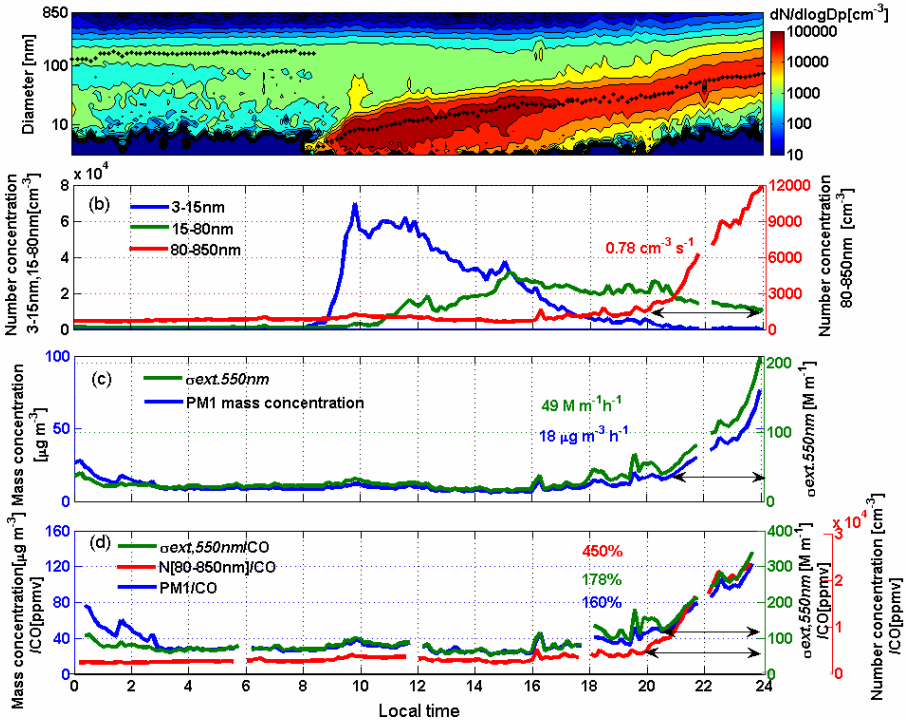

Fig. 9. The number size distribution at SDZ on 13 March 2008 and mode diameter (dots) **(a)**, evolution of the number concentration of 3–15 nm, 15–80 nm and 80–850 nm, respectively **(b)**, evolution of $\sigma_{ext,550nm}$, extinction coefficient at 550 nm and PM_1 mass concentration calculated from TDMPS data **(c)** and the normalized number concentration of 80–850 nm, PM_1 mass concentration and $\sigma_{ext,550nm}$ by the concentration of CO.

ACPD
10, 25205–25242, 2010

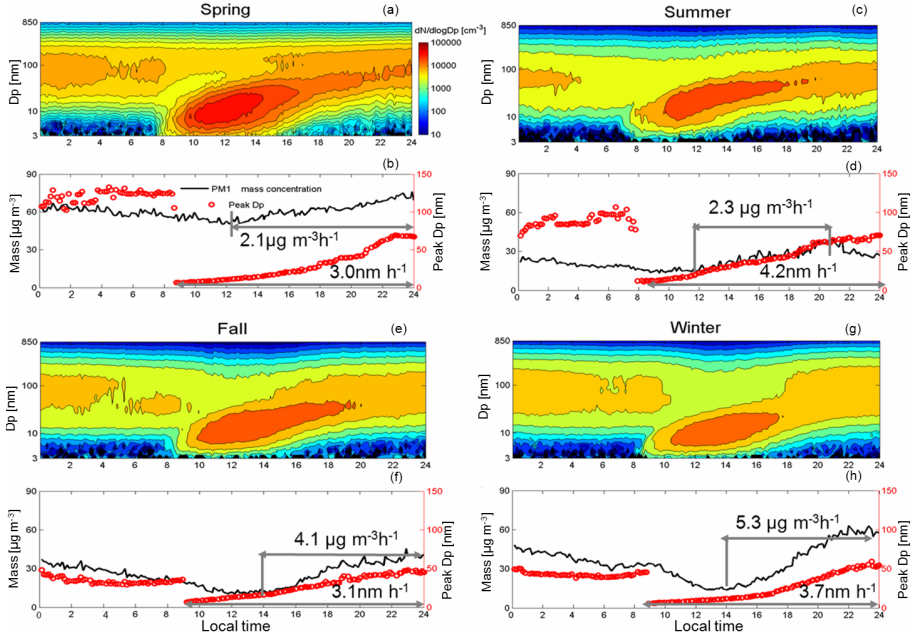

Fig. 10. The evolutions of the particle size distributions **(a, c, e, g)**, PM_1 mass concentration derived from number size distributions and mean diameter of the dominating mode from mode fitting to the average particle size distributions **(b, d, f, h)** from only NPF event days in four seasons.

ACPD
10, 25205–25242, 2010